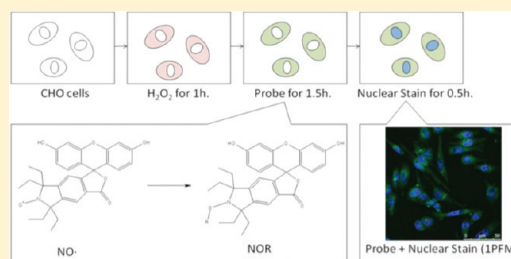# Two-Photon Fluorescence Microscopy Imaging of Cellular Oxidative Stress Using Profluorescent Nitroxides

Hyo-Yang Ahn,[†] Kathryn E. Fairfull-Smith,[§] Benjamin J. Morrow,[§] Vanessa Lussini,[§] Bosung Kim,[†] Mykhailo V. Bondar,[⊥] Steven E. Bottle,[§] and Kevin D. Belfield*[,†,‡]

[†]Department of Chemistry, and [‡]CREOL, The College of Optics and Photonics, University of Central Florida, P.O. Box 162366, Orlando, Florida 32816-2366, United States

[§]ARC Centre of Excellence for Free Radical Chemistry and Biotechnology, Faculty of Science and Technology, Queensland University of Technology, GPO Box 2434, Brisbane, QLD, 4001, Australia

[⊥]Institute of Physics, National Academy of Sciences, Prospect Nauki 46, Kiev 03028, Ukraine

S *Supporting Information*

ABSTRACT: A range of varying chromophore nitroxide free radicals and their nonradical methoxyamine analogues were synthesized and their linear photophysical properties examined. The presence of the proximate free radical masks the chromophore's usual fluorescence emission, and these species are described as profluorescent. Two nitroxides incorporating anthracene and fluorescein chromophores (compounds **7** and **19**, respectively) exhibited two-photon absorption (2PA) cross sections of approximately 400 G.M. when excited at wavelengths greater than 800 nm. Both of these profluorescent nitroxides demonstrated low cytotoxicity toward Chinese hamster ovary (CHO) cells. Imaging colocalization experiments with the commercially available CellROX Deep Red oxidative stress monitor demonstrated good cellular uptake of the nitroxide probes. Sensitivity of the nitroxide probes to H_2O_2-induced damage was also demonstrated by both one- and two-photon fluorescence microscopy. These profluorescent nitroxide probes are potentially powerful tools for imaging oxidative stress in biological systems, and they essentially "light up" in the presence of certain species generated from oxidative stress. The high ratio of the fluorescence quantum yield between the profluorescent nitroxide species and their nonradical adducts provides the sensitivity required for measuring a range of cellular redox environments. Furthermore, their reasonable 2PA cross sections provide for the option of using two-photon fluorescence microscopy, which circumvents commonly encountered disadvantages associated with one-photon imaging such as photobleaching and poor tissue penetration.

INTRODUCTION

Since the 1960s, the chemistry of nitroxides has been widely investigated due to their unique physical and chemical properties.[1,2] Nitroxide radicals have been commonly utilized for spin trapping and spin labeling applications in electron paramagnetic resonance (EPR) spectroscopy[3] and for monitoring cellular redox processes.[4] Nitroxides are also effective antioxidants in biological systems due to their ability to react with superoxide radicals.[5] Superoxide, one of the main reactive oxygen species produced in the cell, is a significant contributor to cellular levels of *oxidative stress*, a term which describes an imbalance in the concentrations of pro- and antioxidants. Oxidative stress results in cellular damage due to the generation of peroxides and free radicals and has been implicated in cardiovascular aging,[6] Parkinson's disease,[7] and Alzheimer's disease.[8] Nitroxides have shown significant potential as small molecule antioxidants in mammalian cells due to their broad distribution and ability to react with and detoxify harmful radical species.[9−11]

As a result of their reactivity toward biologically relevant radicals, nitroxides have also found utility as sensitive probes for reactive oxygen species. Profluorescent nitroxides,[12] which contain a fluorophore closely linked to a nitroxide moiety, display significantly reduced fluorescence due to efficient quenching of the excited electronic state of the fluorophore by the nitroxide radical. Upon reduction, oxidation, or radical trapping, however, normal fluorophore emission is enabled, making these compounds very sensitive probes for the detection of free radical species. Profluorescent nitroxides have been utilized as probes for the detection of the biologically relevant reductant ascorbic acid[13−17] and the biologically important radical superoxide.[18] Glutathionyl radicals have also been detected by an associated fluorescence increase of acridine nitroxide profluorescent probes in cells.[19,20] More recently, a fluorescein-based nitroxide probe was combined with flow cytometry to highlight the difference between healthy cells and those undergoing oxidative stress.[21] Depending on the chromophore moiety present within the profluorescent nitroxide species, the absorption and emission wavelengths of these probes can be tuned to match

specific applications, such as cellular imaging. Thus, profluorescent nitroxides are extremely useful tools for monitoring and imaging changes in the redox status of the cellular environment; however, their use as probes for two-photon fluorescence microscopy imaging has previously not been investigated.

Two-photon fluorescence microscopy is a three-dimensional imaging technique involving the nonlinear excitation of fluorophores.[22] The application of two-photon excitation to fluorescence microscopy offers several advantages over conventional imaging techniques.[23,24] It facilitates deep tissue penetration with unparalleled spatial resolution and also dramatically reduces fluorophore photobleaching, which is a common drawback of fluorescence microscopy.

Chang and Cho et al.[25] have demonstrated the power of employing two-photon imaging of reactive oxygen species by developing the first two-photon probe for H_2O_2. Using a carbamate detection mechanism, H_2O_2 was imaged in live cells and in living tissue at depths ranging from 90 to 180 μm. The use of two-photon imaging enabled detection of the probe with single cell resolution at a depth of 120 μm.

Considering the inherent advantages associated with two-photon imaging as showcased by Chang and Cho et al.[25] and the demonstrated ability of nitroxides to detect reactive oxygen species, we report here the first examples of two-photon profluorescent nitroxides for the detection and imaging of reactive oxygen species. The paramagnetic nitroxide present in these probes behaves as a two-photon fluorescence off–on switch for detection of ROS. Herein, we report a range of novel profluorescent nitroxides along with their photophysical properties and examine their applicability as powerful tools to probe the cellular redox environment using two-photon fluorescence microscopy (2PFM) imaging. The two-photon measurements reported here demonstrate the potential use of these probes for imaging the redox environment in living tissues and provide insights into the role of oxidative stress in a range of complex disease states such as cancer, inflammation, and neurodegenerative disorders.

■ EXPERIMENTAL SECTION

Synthesis. The synthesis of compounds **1–8** has been previously reported.[26] The dansyl-linked nitroxides **9**, **11**, **13**, and **15** were prepared from dansyl chloride and the corresponding amino- or hydroxy-substituted nitroxide using standard coupling techniques, and the corresponding methoxyamines **10**, **12**, **14**, and **16** were prepared by reaction of the appropriate nitroxide with methyl radicals formed using Fenton chemistry.[27] The perylene diimide-linked dinitroxide **17** was prepared from 3,4,9,10-perylenetetracarboxylic dianhydride and 5-amino-1,3,3-tetramethylisoindolin-2-yloxyl, and the methoxyamine derivative **18** was prepared using Fenton chemistry from nitroxide **17** using established procedures.[28,29] The novel tetraethyl fluorescein nitroxide **19** was synthesized using a method similar to that reported for the synthesis of its tetramethyl analogue.[21] The synthesis and corresponding characterization data are reported in the Supporting Information for each new compound (**9–20**).

Linear Optical Properties. Linear absorption was measured with an Agilent 8453 UV–vis spectrophotometer. Fluorescence emission and excitation spectra were measured using a PTI Quantamaster spectrofluorimeter equipped with a Hamamatsu R928 photomultiplier tube (PMT). Emission spectra were measured in cyclohexane, CH_2Cl_2, or water, depending on the solubility of the compound. Excitation anisotropy spectra were measured with two Glan-Thomson polarizers in an L-format method in high viscosity solvent (glycerol, Acros) to avoid reorientation, and in low concentration solutions ($C \sim 10^{-6}$ M) to avoid reabsorption.[30] Fluorescence quantum yields for compounds

1–8 were obtained from measurements at five different concentrations in cyclohexane using the following equation:

$$\Phi_{F\ sample} = \Phi_{F\ standard} \times (Abs_{standard}/Abs_{sample})$$
$$\times \left(\sum F_{sample} / \sum F_{standard} \right)$$

where Abs and F denote the absorbance and fluorescence intensity, respectively, and $\sum F$ denotes the peak area of the fluorescence spectra, calculated by summation of the fluorescence intensity. Anthracene ($\Phi_F = 0.36$) was used as a standard, and excitation was performed at 340 nm. Extinction coefficients were calculated from the obtained absorbance spectra. Fluorescence quantum yields for the other compounds were similarly determined.

Lifetime measurements were performed using a tunable Ti:sapphire laser system (Coherent Verdi-V10 and MIRA 900, pulse duration ~200 fs/pulse (fwhm), and repetition rate 76 MHz) coupled with a second harmonic generator. The polarization of the excitation beam was linear and oriented by the magic angle to avoid molecular reorientation effects. A broad band-pass filter (400 to 600 nm, or 500 to 700 nm, depending on the emission range of a compound) was placed in front of an avalanche photodiode detector (APD, PicoQuant GmbH, LSM_SPAD). Data was acquired with a PicoQuant time-correlated single photon counting system, PicoHarp300 (see the Supporting Information). The optical density of all the solutions did not exceed 0.12 at the excitation wavelength to avoid reabsorption. Measurements were conducted in 10 mm path length quartz cuvettes at room temperature.

Nonlinear Optical Properties. Two-photon absorption (2PA) measurements were performed using a Coherent Legend Elite system (amplified Ti:sapphire system) and an optical parametric generator/amplifier (Coherent OPerA Solo), providing laser pulses of 100 fs (fwhm) duration with 1 kHz repetition rate (see the Supporting Information). The system was coupled with a PTI Quantamaster spectrofluorimeter and R928 PMT. The 2PA spectrum was determined over a broad spectral region from 580 to 1020 nm by the two-photon induced fluorescence method using 10^{-5} M $\leq C \leq$ 10^{-3} M concentration. Solutions were in a 10 mm quartz cuvette at room temperature relative to rhodamine B.[31] All linear and nonlinear measurements were carried out in spectroscopic grade solvents.

Cell Assays. *Micelle Encapsulation.* A concentrated micelle stock solution was prepared using 1 mg/mL of the dye by using a small amount of CH_2Cl_2 to dissolve the dye. Water was added with 2 wt % of surfactant (Pluronic F 127 Prill, BASF Corporation) and stirred overnight. The crude solution was filtered before using. The concentration of the micelle-encapsulated probe stock solution was determined via UV–vis spectrophotometry using the molar absorptivity.

Cell Lines. Chinese hamster ovary (CHO) cells were purchased from America Type Culture Collection (ATCC, Manassas, VA). All cells were incubated at 37 °C in a 95% humidified atmosphere containing 5% CO_2 in cell media (RPMI medium with 10% fetal bovine serum, 1% Pen Strep (penicillin–streptomycin, Invitrogen, Carlsbad, CA), and 0.75 g of sodium bicarbonate).

Cytotoxicity Assay. CHO cells were prepared for cell viability studies in 96-well plates (4×10^3 cells per well that were incubated in 90 μL). The cells were incubated for an additional 20 h with dyes encapsulated in micelles (**7** and **8**) and aqueous solution (**17** and **18**) in different concentrations. Subsequently, 10 μL of MTS assay (CellTiter 96 Aqueous One Solution reagent) was added into each well, followed by further incubation for 4 h at 37 °C. The relative viability of the cells incubated with dyes to untreated cells was determined by measuring the MTS-formazan absorbance on a microplate reader (Spectra Max M5, Molecular Devices) at 538 nm with subtraction of the absorbance of the cell-free blank volume at 538 nm.[32,33] The results from the three individual experiments were averaged.

Cell Culture and Fixing. CHO cells were placed onto poly-D-lysine-coated glass coverslips (12 mm, #1) in 24-well plates, 3×10^4 cells per well (0.5 mL), and the cells were incubated for 48 h before further use. Diluted hydrogen peroxide (0.1 mL, 6% solution, Fisher

4722

dx.doi.org/10.1021/ja210315x | J. Am. Chem. Soc. 2012, 134, 4721–4730

Table 1. Linear Photophysical Properties of the Nitroxide Radicals and Their Methoxyamine Derivatives[a]

	cyclohexane						dichloromethane							glycerol
	$\lambda_{Abs.}^{max}$	$\lambda_{Em.}^{max}$	$\Delta\lambda$	φ_{FL}	τ_{FL} (ns)	χ^2	$\lambda_{Abs.}^{max}$	$\lambda_{Em.}^{max}$	$\Delta\lambda$	φ_{FL}	φ_{FL}(NOMe/NO·)	τ_{FL} (ns)	χ^2	R
1	374	411	37	0.041	0.48	0.92	376	416	40	0.059		0.05	0.98	
2	374	411	37	0.89	5.02	0.99	376	415	39	1.0	16.9	5.44	0.99	0.13
3	374	418	44	0.021	0.34	0.99	375	430	55	0.017		0.07	0.91	
4	374	409	35	0.85	5.3	0.99	375	414	39	0.97	57.1	6.1	0.99	0.21
5	452	475	23	0.025	0.16	0.99	469	481	12	0.015		0.09	0.99	
6	453	475	22	0.95	2.78	0.99	470	482	12	1.0	66.7	2.95	0.99	0.18
7	452	473	21	0.04	0.35	0.90	465	478	13	0.011		0.10	0.98	
8	452	474	22	0.95	2.9	0.99	466	480	14	0.75	68.2	3.1	0.99	0.31
9	344	469	125	0.066	0.61	0.92	349	513	164	0.076		2.4	0.97	
10	342	471	129	0.67	8.2	0.94	346	510	164	0.54	7.1	13.6	0.97	0.38
11	341	463	122	0.033	0.44	0.99	345	499	154	0.022		0.6	0.99	
12	339	460	121	0.77	8.7	0.98	343	498	155	0.58	26.4	14.8	0.96	0.38
13	345	471	126	0.048	0.75	0.99	355	532	177	0.126		2.76	0.99	
14	342	469	127	0.64	11.5	0.98	353	527	174	0.45	3.6	11.2	0.99	0.36
15	338	455	117	0.037	0.57	0.99	347	511	164	0.109		0.99	0.99	
16	341	458	117	0.53	9.8	0.98	347	510	163	0.75	6.9	15.5	0.97	0.37
17	insoluble						527	534	7	0.009		0.12	0.99	
18	insoluble						526	534	8	0.25	27.8	1.56	0.99	0.39
							water							
19	insoluble						491	511	20	0.14		0.38	0.99	
20	insoluble						490	540	50	0.92	6.6	3.91	0.99	0.40

[a] λ_{Abs}^{max} and λ_{Abs}^{max} refer to absorption and emission maximum, respectively, $\Delta\lambda$ denotes the Stokes shift, φ_{FL} denotes fluorescence quantum yield, τ_{FL} (ns) is fluorescence lifetime, χ^2 refers to correlation coefficient φ_{FL} (NOMe/NO·) is the fluorescence quantum yield ratio of the methoxy (NOMe) to nitroxide (NO·), and R is fluorescence excitation anisotropy.

Scientific, diluted with PBS buffer) was added to induce oxidative stress (to generate free radical species), and the cells were incubated for 1 h and then washed twice with PBS. The filtered stock solution of the probe was then diluted with growth medium, RPMI-1640 with 1% Pen Strep and 0.75 g of sodium bicarbonate (0.5 mL), and then incubated for 1.5 h. The cells were incubated for additional 30 min for staining with commercial dyes individually. The stains used were 5 µg/mL of Hoechst 33285 (see Supporting Information) and 5 µM CellROX Deep Red reagent. After incubation, the cells were washed with phosphate-buffered solution (PBS) five times and fixed using 3.7% formaldehyde solution for 15 min at 37 °C. Then freshly prepared NaBH₄ (1 mg/mL) solution in PBS (PBS pH = 7.4, with a couple of drops of 0.1 M NaOH = pH 8) was added to each well (0.5 mL/well) for 15 min and washed with PBS (×3), and this procedure was repeated once more. The plates were then washed with PBS (×2) and water (×1). NaBH₄ was added to reduce autofluorescence (a general protocol) of the fixing medium. No fluorescence was observed in controls in which no H₂O₂ was added, only incubation with the nitroxide probe, see, e.g., Figures 6a and 7a. Results using RPMI or RPMI with serum media were essentially the same. Finally, the glass coverslips were mounted using Prolong Gold mounting media (Invitrogen) for microscopy.

One- and Two-Photon Fluorescence Microscopy (1PFM and 2PFM) Imaging. A Leica TCS SP5MP confocal microscope system coupled to Coherent Chameleon Vision S Ti:sapphire laser (~70 fs (fwhm), 90 MHz repetition rate) was used for one-photon fluorescence microscopy (1PFM) and 2PFM imaging with a 63× water immersion objective (Leica 506279). Visible lasers in the TCS SP5 system were employed for 1PFM while the Coherent Chameleon system was used for 2PFM imaging. Leica LAS AF software was used for capturing and processing images. The excitation wavelength for nitroxides 7 and 17 was 458 nm using an argon laser, while emission was collected from 500 to 600 nm. A HeNe laser (633 nm) was used for exciting the commercial CellROX Deep Red probe while collecting the emission between 650 and 750 nm. Each image was obtained frame by frame at different wavelengths.

■ RESULTS AND DISCUSSION

Synthesis and Physical Properties of Nitroxides. The nitroxide probes were prepared by the reaction of dansyl chloride with the appropriate amino nitroxide in DCM in the presence of base to give the desired dansyl-linked nitroxides 9, 11, 13, and 15 in good yield (65−85%). The methyl ether analogues 10, 12, 14, and 16 were obtained using Fenton chemistry by the reaction of the nitroxides 9, 11, 13, and 15 with methyl radicals generated from dimethyl sulfoxide and hydrogen peroxide. The absorbance spectra and extinction coefficients of the prepared compounds were characteristic of the dansyl fluorophore (Table 1). A comparison of the fluorescence of the nitroxides and their corresponding methoxyamine analogues revealed a substantial fluorescence suppression (10−23 fold) arising from the presence of the nitroxide radical. This effect was confirmed by the measured quantum yields shown in Table 1.

Linear Photophysical Properties. A relatively comprehensive investigation of the linear photophysical properties (Table 1) of 10 pairs of nitroxide radicals and their corresponding methoxyamine analogues (Figure 1) was conducted. Most compounds were soluble in cyclohexane (CHX) and dichloromethane (CH₂Cl₂). Perylene derivatives 17 and 18 were insoluble in CHX. Hence, spectroscopic studies for these compounds were conducted in CH₂Cl₂. Finally, because of their water solubility, measurements of the fluorescein derivatives 19 and 20 were carried out in water. The photophysical properties for diphenylanthracene derivatives (1−4) and bis(phenylethynyl) derivatives (5−8) have been previously reported.[26] Herein, further investigation was performed to determine their feasibility as probes for bioimaging. Diphenylanthracene derivatives 1−4 exhibited absorption maximum at ca. 375 nm in both CHX and CH₂Cl₂. The emission maxima were ca. 410 and 430 nm in CHX and CH₂Cl₂, respectively (see Supporting Information for absorption and emission spectra). As expected, there was a large Stokes shift (up to 55 nm) in the more polar solvent. Bis(phenylethynyl) derivatives 5−8 had absorption maxima of 452 and 465 nm in CHX and CH₂Cl₂, respectively. Emission maxima were 475 and 480 nm in CHX and CH₂Cl₂, respectively. Two types of dansyl
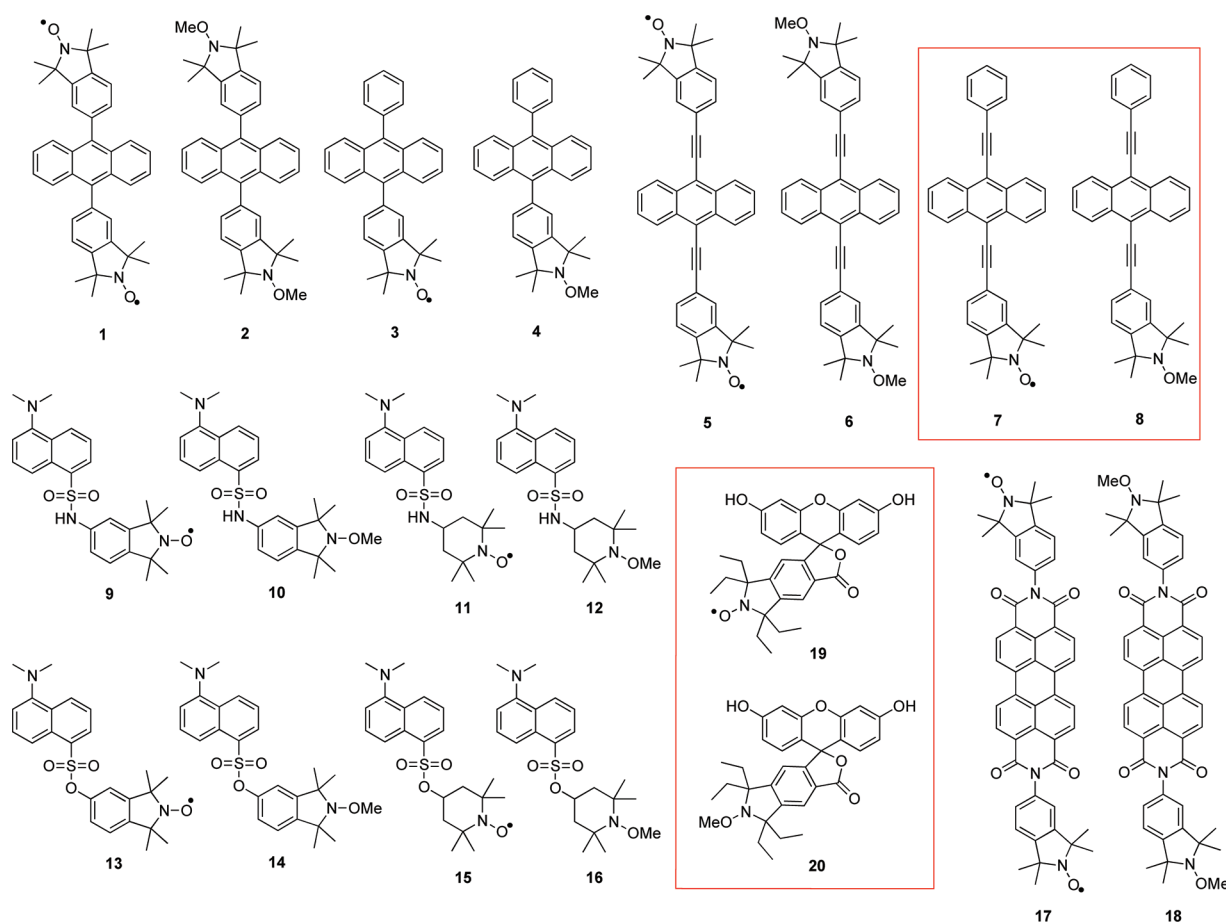
Figure 1. Molecular structures of nitroxide and methoxyamine derivatives.

derivatives were prepared; dansyl sulfonamides **9−12** and dansyl sulfonates **13−16**. The main absorption and emission maxima for both types were ca. 340 and 470 nm, respectively, in CHX, and 350 and 510 nm, respectively, in CH_2Cl_2. The absorption and emission maxima of the perylene derivatives **17** and **18** were 526 and 534 nm in CH_2Cl_2, respectively, while those for the fluorescein derivatives **19** and **20** were at 490 and ca. 520 nm, respectively.

The fluorescence quantum yields (φ_{FL}) of nitroxides (Table 1) were low, starting from as little as 0.009 (**17**) and reaching 0.126 (**13**), while the φ_{FL} of the nonradical methoxyamine (NOMe) derivatives were higher starting from 0.25 (**18**) and reaching 1.0 (**2**). The ratio of φ_{FL} for the nitroxides and their corresponding nonradical methoxyamines was relatively large for the diphenylanthracene derivatives (**1−4**) and for the bis(phenylethynyl) derivatives (**5−8**) displaying >50-fold increase in brightness (i.e., **7** and **8**, φ_{FL} = 0.011 and 0.75, respectively, giving a 68 fold increase, and for **3** and **4**, the ratio was 57). The φ_{FL} ratio of the nitroxide compared to the non-radical methoxyamine derivative models the relative fluorescence increase that would occur when a nitroxide reacts with reactive oxygen species generated in the cell. Dansyl sulfonamides **9−12** and dansyl sulfonates **13−16** exhibited up to ~25-fold increase (i.e., **11** and **12**, φ_{FL} = 0.022 and 0.58, respectively, φ_{FL}(NOMe/NO·) = 26). Because the fluorescence lifetime (τ) is proportional to φ_{FL}, the nitroxides display a significantly shorter τ than the NOMe derivatives (e.g., τ for **1** and **2** in dichloromethane = 0.05 and 5.44 ns, respectively). As a result, the trends for the pairs of nitroxide radical and

methoxyamine derivatives were as follows: (1) the fluorescence quantum yield of the methoxyamines were up to almost 70-fold higher than the corresponding nitroxide (see, e.g., **7** vs **8** and **5** vs **6**), and (2) the measured fluorescence lifetimes correlated well with the calculated fluorescence quantum yields. Notably, the lifetimes of the methoxyamines were up to 2 orders of magnitude greater than the corresponding nitroxide, (e.g., **1** and **2**). Paramagnetic species are recognized as fluorescence quenchers with the decrease in fluorescence arising from rapid excited-state intersystem conversion allowed by changes in the spin multiplicity of the electronic states followed by non-radiative energy loss.[34] However, once this paramagnetic character is removed, i.e., through conversion to the methoxyamine derivative, high fluorescence efficiency is restored as demonstrated by the large fluorescence quantum yields for the non-radical alkylated analogues.

The diphenylanthracene **1−4** and dansyl derivatives **9−16** possess not only short wavelength absorption bands, but also exhibit low two-photon absorptivity.[35] Perylene derivatives **17** and **18** possess a longer wavelength absorption maximum, and the φ_{FL}(NOMe/NO·) ratio is relatively high. However, the fluorescence quantum yield of the corresponding methoxy-amine derivative **18** was lower than that observed for other methoxyamines. Of the bis(phenylethynyl) derivatives, compounds **5** and **7** are promising candidates for two-photon excitation imaging probes. Nitroxide **7** was selected because the monofunctionality simplifies analyses relative to dinitroxide **5**, and its φ_{FL}(**8** NOMe/**7** NO·) ratio was high (~70 fold). Though the φ_{FL}(**20** NOMe/**19** NO·) ratio for fluorescein

derivatives **19** and **20** was only 6.6, their absorption and emission were at relatively long wavelengths, and they were also water-soluble, making them reasonable candidates for bioimaging. Therefore, due to their high fluorescence quantum yields along with 2PA spectra and cross sections, bis(phenylethynyl) derivative **7** and the fluorescein derivative **19** were examined as potential probes for two-photon fluorescence bioimaging.

Nonlinear Optical Properties. When exposed to free radical species, such as the products of oxidative damage in cells, nitroxides may trap other free radicals, typically forming alkoxyamine (NOR) species. They may also be metabolized to nonradical hydroxylamines (i.e., R = H) at rates reflecting the oxidative status of the cell.[21] Figure 2 shows the potential
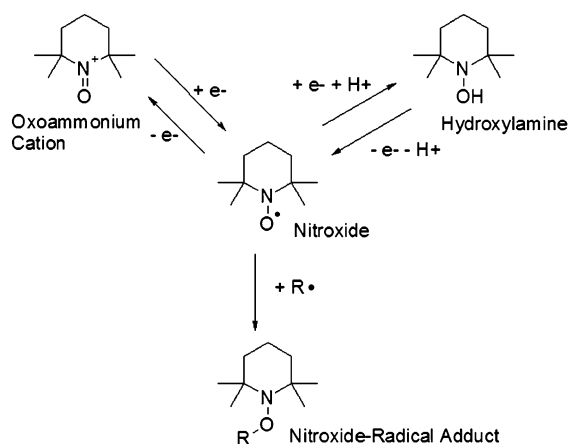
Figure 2. Possible reactions of nitroxides in biological systems.[36]

transformations of nitroxides in biological systems.[10,36] Fluorophore nitroxide compounds typically possess very low fluorescence quantum yields. On the other hand, their related diamagnetic adducts (R₂NOR) fluoresce normally. Thus, the presence of the nitroxide can serve as a 'switch' for the fluorophore, turning off the fluorescence. Switching on the fluorescence would occur following the reaction of the nitroxide with another radical species or alternatively through redox chemistry (oxidation/reduction) to give diamagnetic, nonquenching species. Therefore, although the profluorescent nitroxide is incubated with cells, the methoxyamine derivative is also very useful, as it serves as a model of the fluorescent reaction products that are detected. Consequently, it is important to examine the two-photon absorption spectra of the methoxyamine derivatives, as this provides insight into the behavior of switched-on probe molecules.

Figure 3 displays four different spectra: absorption (black line, normalized spectra), emission (blue, normalized spectra), anisotropy (green), and two-photon absorption (2PA) cross section (half-filled red circle). The 2PA cross section unit of measure is a value referred to as a GM unit (1 GM (Göppert Meyer) = 10^{-50} cm^4 s/photon^{-1}). The 2PA spectra were recorded in 20 nm increments from 590 to 1030 nm corresponding to the top *X*-axis and right *Y*-axis.

The 2PA cross sections of methoxyamine derivatives **8** and **20** were measured using a Coherent Legend Elite system (an amplified Ti:sapphire laser system) coupled with an OPerA Solo optical parametric amplifier (∼100 fs (fwhm), 1 kHz
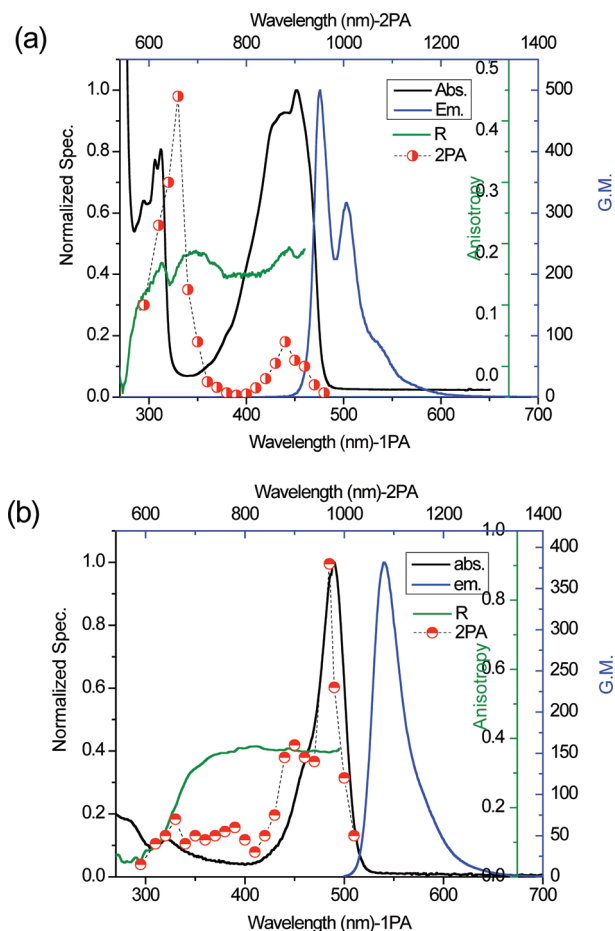
Figure 3. (a) Linear and nonlinear optical spectra of compound **8** and (b) linear and nonlinear optical spectra of compound **20**. In each graph, the linear absorption spectrum is a black line, the emission spectrum is a blue line, fluorescence anisotropy is green, and two-photon absorption (2PA) cross sections are shown as half-filled red circles, respectively.

repetition rate). The equation used for calculation of the 2PA cross section calculation is

$$\delta_{2PA\text{-}s} = \delta_{2PA\text{-}r} \frac{\Phi_r}{\Phi_s} \frac{C_r}{C_s} \frac{\langle F \rangle_s}{\langle F \rangle_r} \frac{n_s}{n_r} \frac{\langle P_r \rangle^2}{\langle P_s \rangle^2}$$

where the subscripts r and s refer to the reference and sample, respectively, Φ is the fluorescence quantum yield, *C* is the concentration, *F* is the integrated area of the main fluorescent band, *n* is the refractive index of the solvent, and *P* is the incident power of the laser. The experimental fluorescence excitation and detection were measured under conditions with negligible reabsorption (close to the cuvette wall).[30] Excitation anisotropy is correlated with the spectral position of various electronic transitions, and can be a very useful tool to estimate the position of 2PA allowed transitions.[37,38] The one-photon allowed S₀−S₁ electronic transition (the maximum of the linear of absorption spectrum) is formally two-photon forbidden according to quantum mechanical selection rules and vice versa. In the case of the bis(phenylethynyl) derivative **8**, the anisotropy spectrum is well correlated with the 2PA cross section data as shown in Figure 3a. The two maxima in the anisotropy spectrum ca. 320 and 440 nm in Figure 3a indicate two possible electronic transitions. The lower energy two-photon transition

is formally forbidden (see discussion below), with 2PA less than that of the higher energy two-photon allowed transition (~500 GM at 670 nm in CHX). Formally, one-photon allowed transitions are two-photon forbidden according to quantum mechanical selction rules. However, this is predicated on a centrosymmetric system. Large organic molecules seldom possess such high symmetry. Thus, for large organic molecules, two-photon absorption into the one-photon allowed transition that is formally two-photon forbidden often occurs due to the relaxed symmetry of the molecule. Such is the case for **8** and **20** due to their low molecular symmetry. The highest 2PA cross section for **20** was ~400 GM at 970 nm in water (pH 8, adjusted with NaOH). Even though the 2PA cross section value of **20** is lower than that of compound **8**, it is still significant due to the desirably long wavelength that can afford deep tissue penetration for ex vivo and in vivo imaging. Hence, **19** is a potentially useful two-photon NIR probe.

Cytotoxicity. A Chinese hamster ovary (CHO) cell line was used for cell viability estimation based on measuring the MTS-formazan absorbance on a plate reader.[32,33] The MTS-formazan absorbance wavelength was observed at 538 nm (not the typical 490 nm) due to overlap with the absorbance of the sample. Hydrogen peroxide was used to induce oxidative stress.[36] Since the concentration of hydrogen peroxide is critical in cell viability, the cytotoxicity of hydrogen peroxide was measured, as shown in Figure 4. Cell viability was reasonable until 100 μM
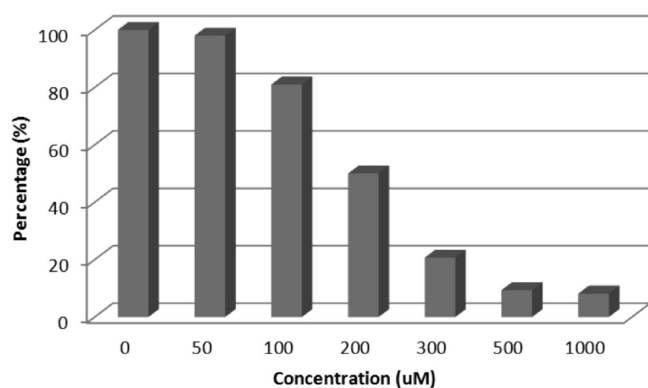

Figure 4. Cell viability evaluation as a function of H_2O_2 concentration after 1 h incubation.

H_2O_2, and the damage increased rapidly, consistent with a previous report.[36] When the concentration of H_2O_2 reached 500 μM, the cell viability was less than 10%.

Compounds **7** and **8** were used to prepare micelle mixtures using 2 wt % of surfactant (Pluronic F 127 Prill) for solubility and biocompatibility. The samples were filtered before use. Cell viability in the presence of H_2O_2 using micelle mixtures of **7** and **8** can be seen in Figure 5a and was above 90% at concentrations up to 50 μM. At concentrations of 5, 10, and 20 μM, nitroxide **7** induces modest enhancement of cell viability, reflecting a potential beneficial antioxidant action at these lower doses.

The use of the nitroxide compounds **7** and **19** as oxidative stress probes was then investigated.[39] Hydrogen peroxide was added just prior to incubation with the nitroxide probe to generate free radical species. Thus, the probe reacts with reactive oxygen species (free radicals) generated by the hydrogen peroxide incubation. The interaction of a nitroxide with hydrogen peroxide does not affect the spin, and so the fluorescence is not switched on by exposure to H_2O_2, as demonstrated by
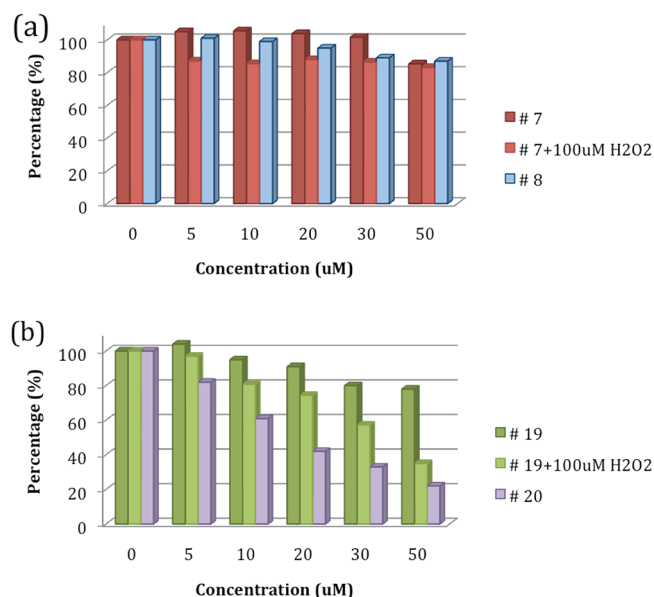

Figure 5. Comparative cell viability of (a) nitroxide 7, 7 + 100 μM H_2O_2, and methoxyamine analogue 8, and (b) nitroxide 19, 19 + 100 μM H_2O_2, and methoxyamine analogue 20.

control reactions for nitroxides **7** and **19** in the presence of 200 μM H_2O_2 with no change observed in the UV−vis absorption spectrum after 4 h. So fluorescence generation from the probes in the cells treated by hydrogen peroxide reflects impacts on the cellular redox status by the peroxide and ROS generated from the cells by the peroxide.

After oxidative stress was generated by incubation of the cells with 100 μM H_2O_2 for 1 h, washing twice with PBS, and the incubation with nitroxide **7** dissolved in RPMI-1640 for 1.5 h, cell viability was determined. The procedure is detailed in the Experimental Section. At the highest dose (50 μM), cell viability decreased by 25% compared to cells which were not treated with compound **7**. However, at doses below 50 μM, at least 80% of the cells remained viable, and at doses of 20 μM or less, cell viability was unchanged or even enhanced. Consequently, at lower doses cell viability does not appear to be an issue for compound **7**, although the optimal concentration for this probe was not determined.

Compounds **19** and **20** were used after dissolving in ultrapure water followed by filtration. Figure 5b illustrates the cell viability using these two probes. Nitroxide **19** exhibited a trend similar to that for **7**, in which the cell viability remained high and even boosted the cell growth at low concentrations of nitroxide. The therapeutic limit for **19** and **20** appeared to be reached with the use of 100 μM H_2O_2 to generate oxidative stress. Above the threshold, the two compounds exhibited a synergistic effect to destroy cells such that the apparent toxicity increased up to 50%. From these experiments, it was determined that 20 μM **19** and 100 μM H_2O_2 can be used for cell culture (to maintain ~80% cell viability within experimental error range). Compound **20**, the methoxyamine analogue of **19**, was relatively toxic to the CHO cells. Hence, only 5 μM dye was utilized to decrease any possible toxicity from the fluorescent radical adducts arising from **19**.

1PFM and 2PFM Images. On the basis of the cell viability results described above along with luminescence quantum yields and 2PA cross sections, 5 μM and 10 μM concentrations
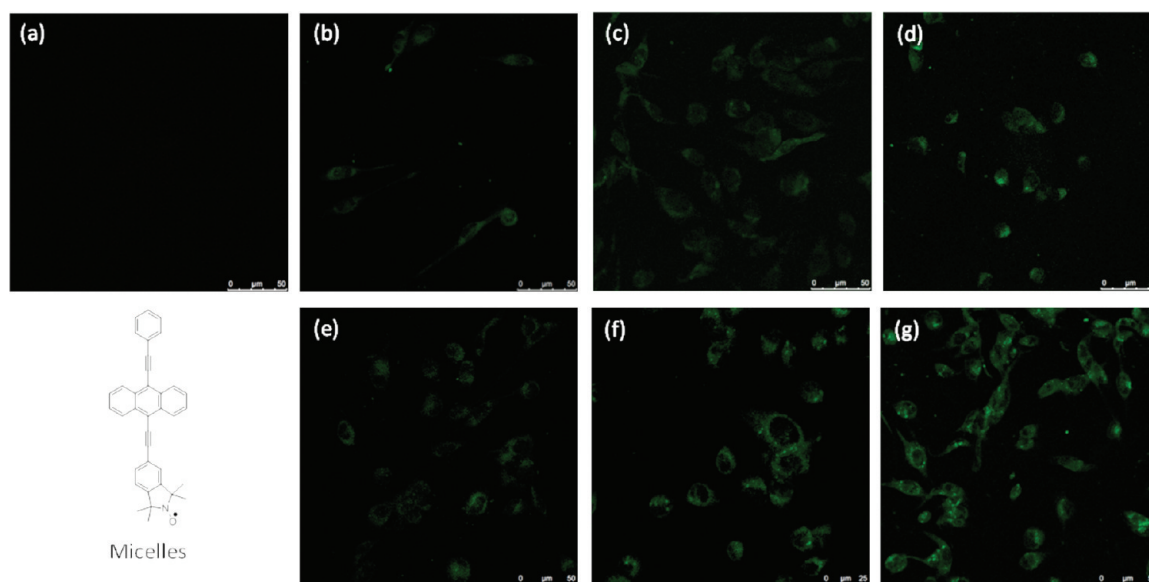
Figure 6. 1PFM image using nitroxide **7** and CHO cells: (a) 0 μM **7** + 0 μM H$_2$O$_2$ (control), (b) 5 μM **7** + 0 μM H$_2$O$_2$, (c) 5 μM **7** + 100 μM H$_2$O$_2$, (d) 5 μM **7** + 200 μM H$_2$O$_2$, (e) 10 μM **7** + 0 μM H$_2$O$_2$, (f) 10 μM **7** + 100 μM H$_2$O$_2$, and (g) 10 μM **7** + 200 μM H$_2$O$_2$.
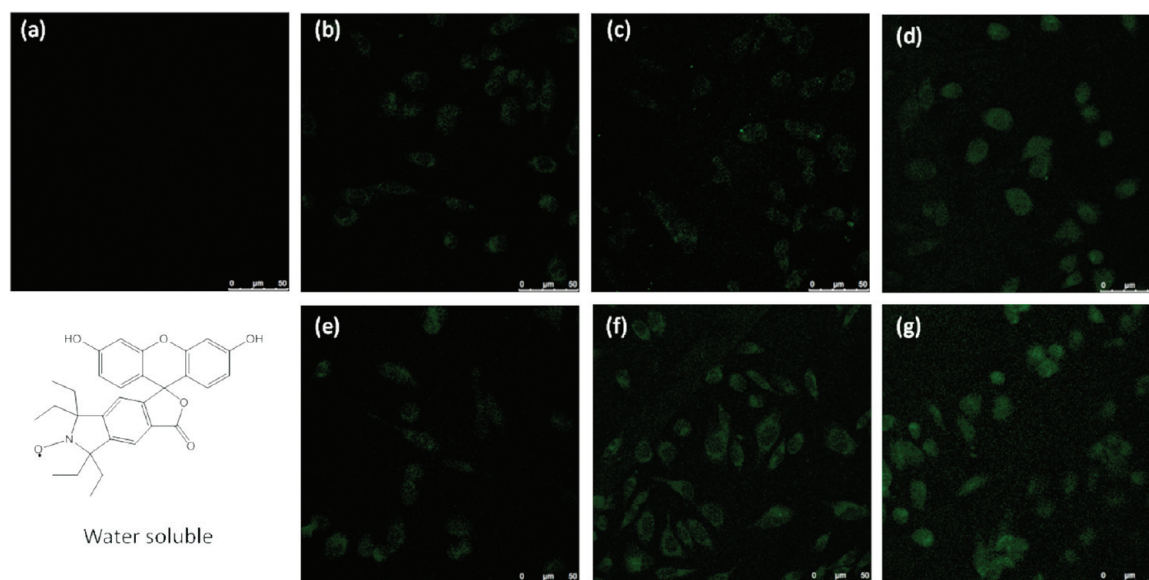
Figure 7. 1PFM imaging with nitroxide **19** and CHO cells: (a) 0 μM **19** + 0 μM H$_2$O$_2$ (control), (b) 5 μM **19** + 0 μM H$_2$O$_2$, (c) 5 μM **19** + 100 μM H$_2$O$_2$, (d) 5 μM **19** + 200 μM H$_2$O$_2$, (e) 10 μM **19** + 0 μM H$_2$O$_2$, (f) 10 μM **19** + 100 μM H$_2$O$_2$, and (g) 10 μM **19** + 200 μM H$_2$O$_2$.

of both nitroxides **7** and **19** were selected for investigation as potential two-photon fluorescent oxidative stress indicators. Nitroxides **7** and **19** were incubated in CHO cells for 2 h. Figure 6 shows the one-photon fluorescence microscopy (1PFM) images of CHO cells incubated with nitroxide **7**. The first row is the comparison of (a) the control (0 μM **7**) vs (b) 5 μM **7**, none of which had any H$_2$O$_2$ added, and increasing concentrations of oxidative stress inducer ((c) 100 μM H$_2$O$_2$ and (d) 200 μM H$_2$O$_2$). The second row shows the structure of the compound, (e) a combination of increased probe concentration and (f and g) increasing concentrations of oxidative stress inducer (H$_2$O$_2$). As anticipated, increases in fluorescence were observed for increases either in the concentration of the probe and H$_2$O$_2$. In Figure 6, panels b–d, a 5 μM concentration of the probe was used while for panels e–g, the probe concentration was 10 μM. The fluoresecence

increased with increasing probe concentration (compare (b) 5 μM and (e) 10 μM). Also, when the concentration of the H$_2$O$_2$ was increased from (c) 100 μM to (d) 200 μM, while maintaining constant probe concentration, an increase in fluorescence was observed. This indicates that the nitroxide probe exhibits brighter fluorescence as a function of concentration (i.e., it is sensitive for the quantity of the probe), and brighter fluorescence is observed at higher oxidative stress levels (i.e., it exhibits sensitivity for oxidative stress). These results support the reaction of species, generated by the action of H$_2$O$_2$ on cells, with profluorescent nitroxide probe **7**, and thereby generating fluorescent NOR analogues (similar to **8**) that may be visualized by 1PFM. Therefore, the result shows that nitroxides **7** and **19** are good oxidative stress indicators.

The response observed for nitroxide **7** was also seen with nitroxide **19**, as shown in Figure 7. The fluorescence intensity
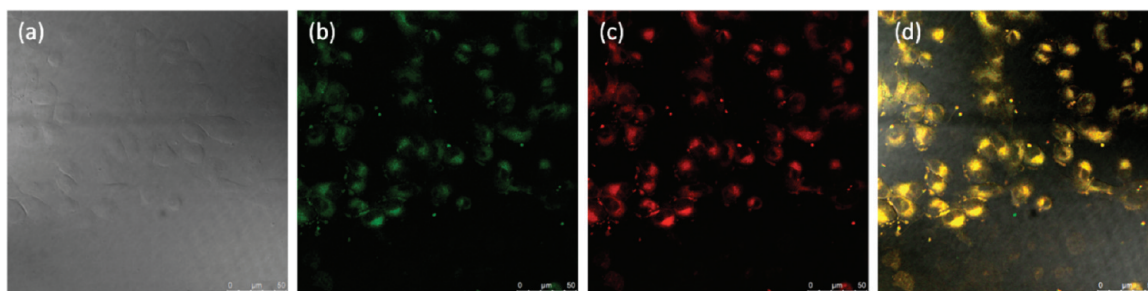
Figure 8. Colocalization study in CHO cells using probe **7** with commercial oxidative stress probe CellROX Deep Red (NOR analogues of **7**: Ex 458 nm/Em 500−600 nm, CellROX Deep Red: Ex 561/Em 580−650 nm): (a) differential interference contrast (DIC) image, (b) cells incubated with 10 μM **7**, (c) cells then incubated with 5 μM CellROX Deep Red, and (d) overlaid images of panels a, b, and c.
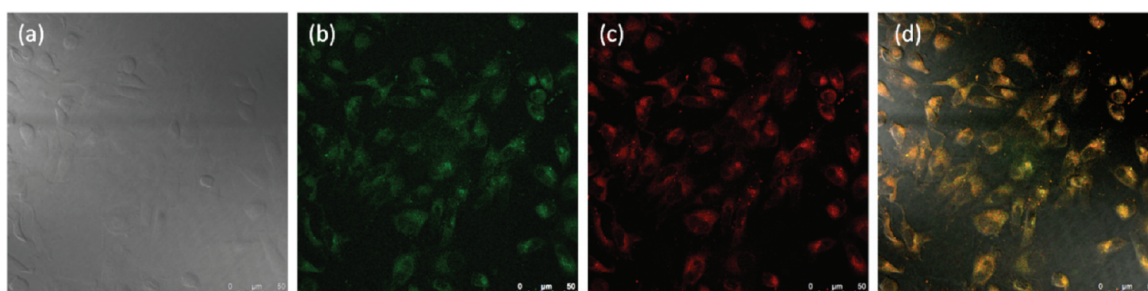

Figure 9. Colocalization study of nitroxide **19** in CHO cells with commercial oxidative stress probe CellROX Deep Red (sample: Ex 458 nm/Em 500−600 nm, CellROX Deep Red: Ex 561/Em 580−650 nm): (a) DIC, (b) incubated with 20 μM **19**, (c) then incubated with 5 μM CellROX Deep Red, and (d) overlaid image of panels a, b, and c.
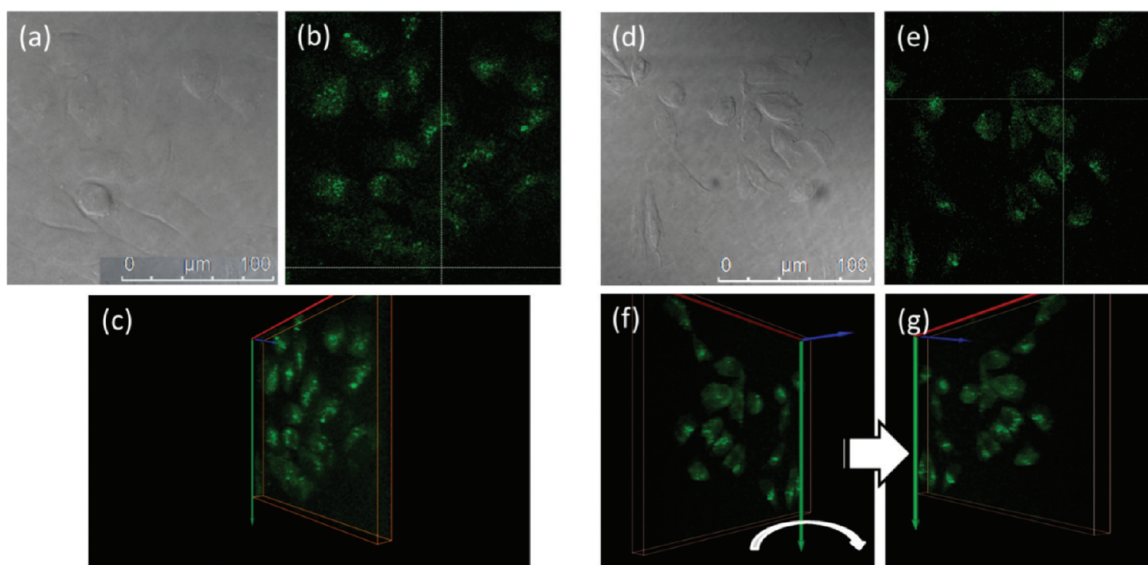

Figure 10. 2PFM images from femtosecond excitation at 900 nm of CHO cells incubated with 10 μM **7** and 200 μM H_2O_2 of (a) DIC, (b) one 2PFM XY optical slice, (c) 2PFM 3D reconstructed image, and incubated with 20 μM **19** and 200 μM H_2O_2: (d) DIC, (e) one 2PFM XY optical slice, (f and g) 2PFM 3D reconstructed image.

increased at higher probe concentration and higher levels of oxidative stress induced through the addition of H_2O_2. Notably previous studies[21] with profluorescent nitroxides have shown that there is no direct interaction between H_2O_2 and the nitroxide at these concentrations, implicating a cellular response mediating this fluorescence increase. Even though the fluorescence quantum yield of nitroxide **19** is significantly higher than nitroxide **7**, the difference in the fluorescence quantum yields of nitroxide **19** and the corresponding NOMe analogue **20** is sufficient and clearly evident in Figure 7 (compare panel b with

panels c and d, or panel e with panels f and g) and is related to the H_2O_2 stress-inducer concentration.

To further support the oxidative stress detection ability of nitroxide **7**, a colocalization study was conducted with commercially available oxidative stress probe CellROX Deep Red reagent.[40] 1PFM images of CHO cells costained with CellROX Deep Red and nitroxide **7** (Figure 8) demonstrated good spatial overlap of the fluorescence from the nonradical NOR derivatives of **7** and CellROX Deep Red (see Figure 8d). The excitation wavelength for imaging of the NOR analogues of **7**

was 458 nm while emission was collected from 500−600 nm. For CellROX Deep Red, the excitation wavelength was 561 nm and emission was collected from 580 to 650 nm.

A similar colocalization study was performed for nitroxide **19** and CellROX Deep Red, as shown in Figure 9. These results indicate good colocalization, supporting the utility of nitroxide **19** as an oxidative stress probe. For a more quantitative comparison, the colocalization coefficient was calculated with ImageJ software (Mander's overlap coefficient). The presumed NOR derivatives of **7** and **19** each had colocalization co-efficients of 96%.

The NOMe analogues of **7** and **19** (**8** and **20**, respectively) had reasonable 2PA cross sections at 900 nm, a good wavelength for 2PFM due to the generally high transparency of biological materials in this region. 2PFM in vitro cell imaging was performed by incubating CHO cells with nitroxide probe **7** or **19** after inducing oxidative stress with H_2O_2 to demonstrate the potential utility of these new probes for 2PFM oxidative stress imaging, as shown in Figure 10.

CONCLUSION

Ten pairs of nitroxides and their nonradical-containing methoxyamine derivatives were examined for their linear and nonlinear photophysical properties. The nitroxides exhibited profluorescent behavior, i.e., their fluorescence quantum yield was significantly higher for the NOMe analogues, while several displayed reasonably high 2PA cross section values above 800 nm, making them good candidates as two-photon fluorescent oxi-dative stress indicators. Because of their linear absorption, nonlinear absorption, and fluorescence properties, nitroxides **7** and **19** were selected for further in vitro cell studies using CHO cells. Cytotoxicity assays indicated that the probes were benign at concentrations suitable for fluorescence microscopy imaging. Colocalization experiments in CHO cells after induction of oxidative stress with H_2O_2 using a commercial indicator of cellular oxidative stress, CellROX Deep Red, demonstrated high colocalization coincidence (96%), supporting the role of the nitroxide probe as a suitable indicator of oxidative stress (and concomitant damage) in vitro. 2PFM imaging was conducted for the first time with a nitroxide oxidative stress probe using probes **7** and **19**. The results from this study provide impetus for the further development of this important class of materials as 2PFM oxidative stress probes and may lead to a new NIR 2PA probe for investigating oxidative stress.

ASSOCIATED CONTENT

Ⓢ Supporting Information

Synthesis and corresponding charaterization data for com-pounds **9−20**, lifetime and 2PA measurement setup, linear photophysical spectra, 1PFM images, ^1H and ^{13}C NMR data, and the full citation for reference 35. This material is available free of charge via the Internet at http://pubs.acs.org.

AUTHOR INFORMATION

Corresponding Author

Belfield@ucf.edu

Notes

The authors declare no competing financial interest.

ACKNOWLEDGMENTS

REFERENCES

(1) Stryer, L.; Griffith, H. O. *Proc. Natl. Acad. Sci. U.S.A.* **1965**, *54*, 1785−1791.

(2) Tebben, L.; Studer, A. *Angew. Chem., Int. Ed.* **2011**, *50*, 5034−5068.

(3) Chen, K.; Glockner, J. F.; Morse, P. D.; Swartz, H. M. *Biochemistry* **1989**, *28* (6), 2496−2501.

(4) Swartz, H. M.; Chen, K.; Pals, M.; Sentjurc, M.; Morse, P. D. II *Magn. Reson. Med.* **1986**, *3*, 169−174.

(5) Samunis, A.; Krishna, C. M.; Riesz, P.; Finkelstein, E.; Rusw, A. *Biol. Chem.* **1988**, *263* (43), 17921−17924.

(6) Raju, S. V. Y.; Barouch, L. a.; Hare, J. M. *Sci. Aging Knowl. Environ.* **2005**, No. 21, re4.

(7) Lipman, T.; Tabakman, R.; Lazarovici, P. *Eur. J. Pharmacol.* **2006**, *549* (1−3), 50−57.

(8) Varadarajan, S.; Yatin, S.; Aksenova, M.; Butterfield, D. A. *J. Struct. Biol.* **2000**, *130* (2−3), 184−208.

(9) Samuni, A. M.; DeGraff, W.; Cook, J. a.; Krishna, M. C.; Russo, A.; Mitchell, J. B. *Free Radical Biol. Med.* **2004**, *37* (10), 1648−1655.

(10) Mitchell, J. B.; Samuni, A.; Krishna, M. C.; DeGraff, W. G.; Ahn, M. S.; Samuni, U.; Russo, A. *Biochemistry* **1990**, *29*, 2802−2807.

(11) Mitchell, J. B.; DeGraff, W.; Kaufman, D.; Krishna, M. C.; Samuni, A.; Finkelstein, E.; Ahn, M. S.; Hahn, S. M.; Gamson, J.; Russo, A. *Arch. Biochem. Biophys.* **1991**, *289*, 62−70.

(12) Blinco, J. P.; Fairfull-Smith, K. E.; Morrow, B. J.; Bottle, S. E. *Aust. J. Chem.* **2011**, *64*, 373−389.

(13) Blough, N. V.; Simpson, D. J. *J. Am. Chem. Soc.* **1988**, *110* (6), 1915−1917.

(14) Lozinsky, E.; Matin, V. V.; Berezina, T. A.; Shames, A. I.; Weis, D. L.; Likhtenshtein, G. I. *J. Biochem. Biophys. Methods* **1998**, *38*, 29−42.

(15) Lozinsky, E.; Novoselsky, A.; Shames, A. I.; Saphier, O.; Likhtenshtein, G. I.; Meyerstein, D. *Biochim. Biophys. Acta* **2001**, *48*, 43−60.

(16) Sato, S.; Suzuki, M.; Soma, T.; Tsunoda, M. *Spectrochim. Acta, Part A* **2008**, *70*, 799−804.

(17) Sato, S.; Tsunoda, M.; Suzuki, M.; Kutsuna, M.; Takido-uchi, K.; Shindo, M.; Mizugushi, H.; Obara, H.; Ohya, H. *Spectrochim. Acta, Part A* **2009**, *71*, 2030−2039.

(18) Medvedeva, N.; Martin, V. V.; Weis, A. L.; Likhtenshten, G. I. *J. Photochem. Photobiol. A* **2004**, *163*, 45−51.

(19) Borisenko, G. G.; Martin, I.; Zhao, Q.; Amoscato, A. A.; Tyurina, Y. Y.; Kagan, V. E. *J. Biol. Chem.* **2004**, *279*, 23453−23462.

(20) Borisenko, G. G.; Martin, I.; Zhao, Q.; Amoscato, A. A.; Kagan, V. E. *J. Am. Chem. Soc.* **2004**, *126*, 9221−9232.

(21) Morrow, B. J.; Keddie, D. J.; Gueven, N.; Lavin, M. F.; Bottle, S. E. *Free Radical Biol. Med.* **2010**, *40*, 67−76.

(22) Denk, W.; Strickler, J. H.; Webb, W. W. *Science* **1990**, *248*, 73−76.

(23) So, P. T. C.; Dong, C. Y.; Masters, B. R.; Berland, K. M. *Annu. Rev. Biomed. Eng.* **2000**, *2*, 399−429.

(24) Mulligan, S. J.; MacVicar, B. A. *Modern Research and Educational Topics in Microscopy*; Formatex: Badajoz, Spain, 2007; Vol. 2, pp 881−889

(25) Chung, C.; Srikun, D.; Lim, C. S.; Chang, C. J.; Cho, B. R. *Chem. Commun.* **2011**, *47*, 9618−9620.

(26) Fairfull-Smith, K. E.; Bottle, S. E. *Eur. J. Org. Chem.* **2008**, *32*, 5391−5400.

(27) Keddie, D. J.; Johnson, T. E.; Arnold, D. P; Bottle, S. E. *Org. Biomol. Chem.* **2005**, *3*, 2593−2598.

(28) Keddie, D. J.; Fairfull-Smith, K. E.; Bottle, S. E. *Org. Biomol. Chem.* **2008**, *6* (17), 3135−3143.

(29) Fairfull-Smith, K. E.; Brackmann, F.; Bottle, S. E. *Eur. J. Org. Chem.* **2009**, *12*, 1902−1915.

(30) *Principles of Fluorescence Spectroscopy*, 3rd ed.; Lakowicz, J. R., Ed.; Springer: Singapore, 2006.

(31) Makarov, N. S.; Drobizhev, M.; Rebane, A. *Opt. Express* **2008**, *16* (6), 4029−4047.

(32) Wang, X.; Nguyen, D. M.; Yanez, C. O.; Rodriguez, L.; Ahn, H.-Y.; Bondar, M. V.; Belfield, K. D. *J. Am. Chem. Soc.* **2010**, *132* (35), 12237−12239.

(33) Wang, X.; Yao, S.; Ahn, H.-Y.; Zhang, Y.; Bondar, M. V.; Torres, J. A.; Belfield, K. D. *Biomed. Opt. Express* **2010**, *1* (2), 11539−11544.

(34) Likhtenstein, G. I.; Ishii, K. *Photochemistry* **2007**, *2*, 871−881.

(35) Chui, C. H.; et al. *Chem. Commun.* **2010**, *46* (20), 3538−40.

(36) DeGraff, W. G.; Krishna, M. C.; Russo, a.; Mitchell, J. B. *Environ. Mol. Mutagen.* **1992**, *19*, 21−6.

(37) Belfield, K. D.; Bondar, M. V.; Hales, J. M.; Morales, A. R.; Przhonska, O. V.; Schafer, K. J. *J. Fluoresc.* **2005**, *15*, 3−11.

(38) Belfield, K. D.; Bondar, M. V.; Kachkovsky, O. D.; Przhonska, O. V.; Yao, S. *J. Lumin.* **2007**, *126*, 14−20.

(39) Emoto, M.; Mito, F.; Yamasaki, T.; Yamada, K.; Sato-Akaba, H.; Hirata, H.; Fujii, H. *Free Radic. Res.* **2011**, *45* (11−12), 1325−32.

(40) Invitrogen. Shedding Light on Oxidative Stress. *BioProbes*, April 2011, Vol. *64*, pp 6−9.

4730

dx.doi.org/10.1021/ja210315x | *J. Am. Chem. Soc.* 2012, 134, 4721−4730